Interference modulation of photoemission from biased metal cathodes driven by two lasers of the same frequency

Cite as: AIP Advances 10, 075301 (2020); doi: 10.1063/5.0010792
Submitted: 14 April 2020 • Accepted: 11 June 2020 •
Published Online: 1 July 2020

Yi Luo,[1] John Luginsland,[1,2] and Peng Zhang[1,a)]

AFFILIATIONS

[1] Department of Electrical and Computer Engineering, Michigan State University, East Lansing, Michigan 48824-1226, USA
[2] Confluent Science, LLC, Albuquerque, New Mexico 87111, USA

[a)] Author to whom correspondence should be addressed: pz@egr.msu.edu

ABSTRACT

We propose to use two lasers of the same frequency to achieve interference modulation of photoelectron emission. Using a quantum mechanical model, we study the time-resolved photoelectron energy spectra and emission current modulation under different laser and dc fields. We find that strong interference modulation of photoemission can be easily achieved with two lasers of the same frequency, due to, on one hand, the straightforward access to the single-frequency laser pairs in experiments and, on the other hand, the low threshold value of the ratio of the laser fields for large modulation depth even with a strong dc field. Our study demonstrates the capability of using interference modulation by single-frequency laser pairs for practical measurements of time-resolved photoelectron energy spectra.

Ultrafast electron emission from nanostructures driven by lasers is of large interest, due to its wide applications, such as time-resolved photoelectron microscopy,[1–5] electron diffraction imaging,[6–9] ultrafast electron sources,[10–13] free-electron lasers,[14,15] attosecond electronic devices,[16–18] and emerging vacuum nanodevices.[19–21] Recently, two-color laser-induced electron emission from nanoemitters[22–28] has drawn strong interest as it provides an attractive platform for modulating photoelectron emission by the relative phase difference between the two lasers. It also shows promise for the potential application of time-resolved photoelectron spectroscopy.[28,29] However, the two-color laser system typically relies on the generation of higher order harmonics of a fundamental laser,[22–26] which, because of its stringent requirements on the experimental setup and its relatively low efficiency, greatly limits the accessibility of the two-color laser system. For higher intensity lasers, harmonic generation becomes increasingly complex and difficult to control.[30,31]

In this work, we propose to utilize two lasers of the same frequency to modulate the photoelectron emission by their relative phase delay. This is motivated by the simple experimental implementation of single-frequency laser pairs, e.g., via a beam splitter with various coating materials to control the reflection and transmission of incident light.[32–35] The two same-frequency lasers may be tuned to have a virtually arbitrary ratio of intensities (in contrast to a small harmonic-to-fundamental intensity ratio in the two-color laser system[22–26]), thus providing a much larger parameter space to assess the interference effect of the two lasers and the induced photoelectron emission. Using a quantum mechanical model,[36] we study the photoemission modulation properties for a dc-biased metal cathode illuminated by two laser fields with the same frequency. We investigate the modulation of photoemission current and the dynamics of multiphoton excited states for different laser fields, wavelengths, cathode materials, and dc bias. Our study demonstrates the capability of measuring the time-resolved photoelectron energy spectra using single-frequency laser pairs.

Under the action of two laser fields $F_1\cos(\omega t)$ and $F_2\cos(\omega t+\theta)$ and a dc electric field F_0, the time-dependent potential barrier near the surface of the cathode reads[27,28,36,37]

$$\Phi(x,t)=\begin{cases}0, & x<0\\ E_F+W_{eff}-eF_0x-eFx\cos(\omega t+\varphi), & x\geq 0,\end{cases} \quad (1)$$

where E_F is the Fermi energy of the metal cathode, $W_{eff} = W - 2\sqrt{e^3F_0/16\pi\varepsilon_0}$ is the effective work function with the Schottky effect,[36] with W being the nominal work function, e is the elementary charge, ε_0 is the free space permittivity, x is the distance away from the cathode surface ($x = 0$), and F is the magnitude of the total laser field due to the two laser fields $F_1\cos(\omega t)$ and $F_2\cos(\omega t + \theta)$,

$$F = \sqrt{(F_1 + F_2\cos\theta)^2 + (F_2\sin\theta)^2}. \quad (2)$$

From Eq. (2), it is clear that the magnitude of the total laser field depends strongly on the phase delay of the two lasers θ, which is expected to provide a similar current modulation to that in the two-color laser setup.[27,28] The resultant phase $\varphi = \arcsin(F_2\sin\theta/F)$, the effect of which becomes important for photoemission only in very short laser pulses when the carrier–envelope phase matters. For laser pulses longer than about 10 cycles, it can be well approximated by continuous-wave excitation for photoemission.[36] Thus, in this study, we ignore the effects of the absolute phase and set $\varphi = 0$ without loss of generality. Based on the exact quantum theory of photoemission,[36,37] the time-averaged normalized emission current density, defined as the time-averaged ratio of the transmitted probability current density over the incident probability current density, $\langle w(\varepsilon, x, t)\rangle = \langle J_t/J_i\rangle$, can be obtained as

$$\langle w(\varepsilon)\rangle = \sum_{n=-\infty}^{\infty}\langle w_n(\varepsilon)\rangle, \quad \langle w_n(\varepsilon)\rangle = \frac{(eF_0\hbar/\sqrt{2m})^{1/3}}{\pi\sqrt{\varepsilon}}|T_n|^2, \quad (3)$$

where $\langle w_n\rangle$ denotes the normalized emission current density through the nth channel with emitted electron energy $\varepsilon + n\hbar\omega$ due to the n-photon contribution, $\hbar$ is the reduced Planck constant, m is the electron mass, and T_n represents the transmission coefficient of electron wave functions, which is calculated from

$$2\sqrt{\varepsilon}\delta(l) = \sum_{n=-\infty}^{\infty} T_n\left[\sqrt{\varepsilon + l\hbar\omega}P_{n(n-l)} + \frac{\hbar}{\sqrt{2m}}Q_{n(n-l)}\right], \quad (4)$$

where $\delta(l)$ is the Dirac delta function, l and n are integers, $P_{nl} = \frac{1}{2\pi}\int_0^{2\pi} p_n(\omega t)e^{-il\omega t}d(\omega t)$ and $Q_{nl} = \frac{1}{2\pi}\int_0^{2\pi} q_n(\omega t)e^{-il\omega t}d(\omega t)$ are the Fourier coefficients, with $p_n(\omega t) = \exp[-(ie^2F_0F/m\hbar\omega^3)\sin\omega t + (ie^2F^2/8m\hbar\omega^3)\sin 2\omega t]r(\alpha_n)$ and $q_n(\omega t) = \exp\left[-(ie^2F_0F/m\hbar\omega^3)\sin\omega t + (ie^2F^2/8m\hbar\omega^3)\sin 2\omega t\right]\left[(eF/\hbar\omega)r(\alpha_n)\sin\omega t + (2mF_0e/\hbar^2)^{1/3}s(\alpha_n)\right]$, where $r(\alpha_n) = Ai(\alpha_n) - iBi(\alpha_n)$, $s(\alpha_n) = iAi'(\alpha_n) + Bi'(\alpha_n)$, and $\alpha_n = -[E_n/eF_0 + (eF/m\omega^2)\cos\omega t](2emF_0/\hbar^2)^{1/3}$ with $E_n = \varepsilon + n\hbar\omega - E_F - W_{eff} - U_p$. Here, Ai and Bi are the Airy functions of the first kind and second kind, respectively, $U_p = e^2F^2/4m\omega^2$ is the ponderomotive energy, and a prime denotes the derivative with respect to the argument. For the special case of zero dc field $F_0 = 0$, the time-averaged normalized emission current density becomes[36,37]

$$\langle w(\varepsilon)\rangle = \sum_{n=-\infty}^{\infty}\langle w_n(\varepsilon)\rangle, \quad \langle w_n(\varepsilon)\rangle = \mathrm{Re}\left(|T_n|^2\sqrt{E_n/\varepsilon}\right), \quad (5)$$

where T_n is still calculated from Eq. (4) with P_{nl} and Q_{nl} unchanged, but with $p_n(\omega t) = \exp[(ie^2F^2/8m\hbar\omega^3)\sin 2\omega t + (ieF\sqrt{2mE_n}/m\hbar\omega^2)\cos\omega t]$ and $q_n(\omega t) = p_n(\omega t)[\sqrt{2mE_n}/\hbar + eF\sin\omega t/\hbar\omega]$. These analytical results in Eqs. (3)–(5) are obtained by solving the time-dependent Schrödinger equation exactly with the potential energy given in Eq. (1) (see Ref. 36 for the detailed derivation). We would like to point out that although the calculation here is equivalent to photoemission using a single laser with varying intensity, our proposed method of using two lasers provides more degrees of freedom for experimental control and also offers the capability of measuring the emitted electron spectra vs time after emission, i.e., time-resolved photoelectron energy spectra.

In Fig. 1, we plot the calculated photoelectron energy spectra as a function of the phase difference between the two lasers θ for different dc fields F_0. The wavelength of both lasers is 800 nm ($\hbar\omega$ = 1.55 eV). The metal is assumed to be tungsten,[10,17,22] with a Fermi energy E_F = 7 eV and a work function W = 4.31 eV. Since most of the electrons emitted from sources are located near the Fermi level,[36,38–41] we choose the electron initial energy $\varepsilon = E_F$ for simplicity. Unless mentioned otherwise, these are the default values for the calculations in this paper. Note with laser fields F_1 = 1.8 V/nm and F_2 = 0.3 V/nm for the special case of $\theta = 0$, the total normalized emission current density in Fig. 1 is $\langle w\rangle = 6.67\times10^{-7}$ and 8.71×10^{-5}, for the DC field F_0 = 0 V/nm and 0.8 V/nm, respectively. Using free-electron theory of metal,[37] we find that the corresponding emission current density is 5.74×10^2 A/cm^2 and 6.75×10^4 A/cm^2, respectively.

When the dc field F_0 is turned off, the dominant emission process is three-photon absorption ($n = 3$) [cf. Figs. 1(a) and 1(e)]. This is consistent with the ratio of the work function of tungsten over the photon energy, $W/\hbar\omega \approx 2.8$. By changing the phase difference θ between the two lasers, the electron emission varies sinusoidally [cf. Figs. 1(a) and 1(c)]. When applying a large dc field F_0 to the cathode, the tunneling emission channels ($n \le 2$) are opened up, as shown in Figs. 1(b) and 1(f). This is because the dc field adequately narrows the surface potential barrier, in addition to the Schottky effect induced barrier lowering, enabling the tunneling emission process. In the case of F_0 = 0.8 V/nm, the dominant emission process is shifted to two-photon absorption. From Figs. 1(c) and 1(d), it is found that the multiphoton excited states ($n \ge 3$) vary with respect to the phase delay θ sinusoidally in the same way, with the maximum at $\theta = 0$ and the minimum at $\theta = \pm\pi$, for both values of dc bias F_0. This is in contrast to the two-color laser induced photoemission, where the dynamics of multiphoton excited states changes under different dc bias F_0 [cf. Figs. 10(g) and 10(f) in Ref. 28]. The one-photon ($n = 1$) absorption and direct tunneling ($n = 0$) process are almost independent of θ for the case of F_0 = 0.8 V/nm, as shown in Figs. 1(d) and 1(f). The sinusoidal modulation in the total emission current density $\langle w\rangle$ is shown in Figs. 2(a) and 2(b), for the case of F_0 = 0 V/nm. When the laser field ratio F_2/F_1 increases, the maximum emission current $\langle w\rangle_{max}$ at $\theta = 0$ increases, while the minimum emission current $\langle w\rangle_{min}$ at $\theta = \pi$ decreases, due to the more profound interference of the two lasers. Figure 2(c) shows the modulation depth, $\Gamma = (\langle w\rangle_{max} - \langle w\rangle_{min})/(\langle w\rangle_{max} + \langle w\rangle_{min})$, as a function of laser field ratio F_2/F_1 under different dc fields F_0. For a given F_0, Γ increases as F_2/F_1 increases, and it reaches the maximum value of 100% when $F_1 = F_2$. It is important to note that, in order to reach a large modulation depth ($\Gamma \ge 90\%$), only a small laser field ratio F_2/F_1 is needed even with a strong dc field, e.g., $F_2/F_1 \le 0.4$ when F_0 = 1 V/nm. The dependence of Γ on the dc field F_0 [Fig. 2(c)] is not monotonic and will be examined further in Fig. 3.

Besides making the surface potential barrier narrower, the dc bias induces a reduction of the barrier height via the image charge effect (or the Schottky effect), which strongly influences the photoemission processes.[28,36] In Fig. 3(a), we compare the emission

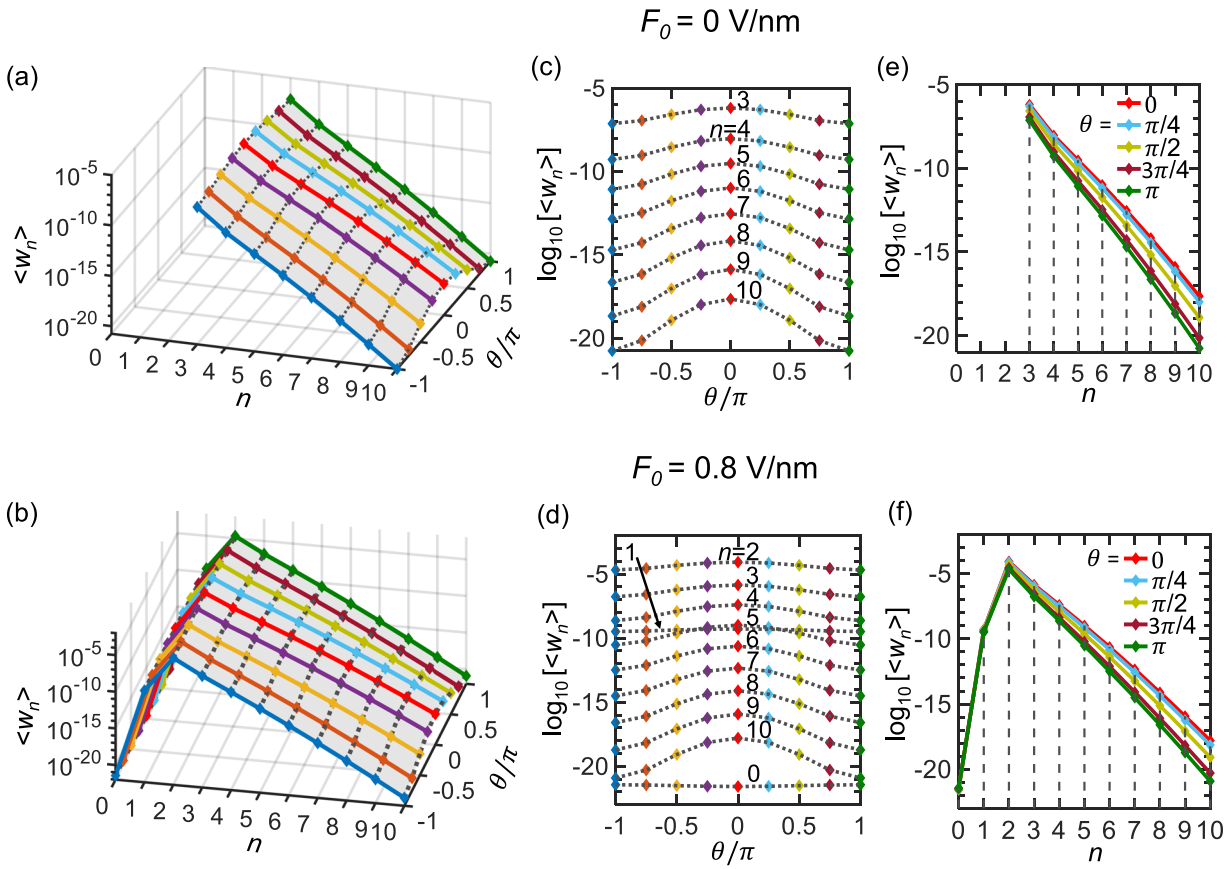

FIG. 1. Time-resolved photoelectron energy spectra. (a) and (b) Energy spectra as a function of the phase difference between the two lasers θ, for dc field (a) F_0 = 0 and (b) F_0 = 0.8 V/nm. (c) and (d) Projections of the spectra in (a) and (b) on the θ–$\langle w \rangle_n$ plane, respectively. (e) and (f) Projections of the spectra in (a) and (b) on the n–$\langle w \rangle_n$ plane, respectively. Here, the laser fields F_1 = 1.8 V/nm and F_2 = 0.3 V/nm (experimental parameters in Ref. 22).

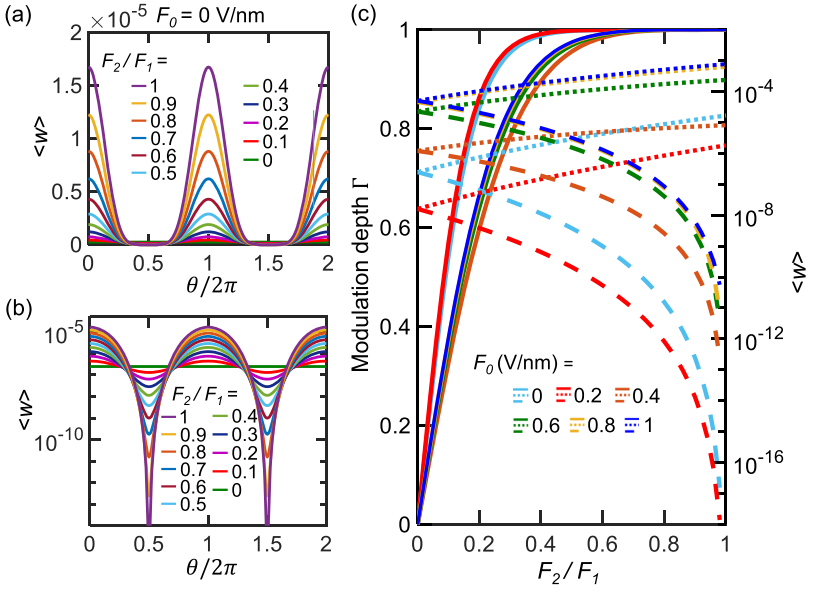

FIG. 2. Photoemission current modulation. (a) Normalized total time-averaged emission current density $\langle w \rangle$ as a function of phase difference θ for different F_2/F_1, when the dc field F_0 = 0. (b) Semilog plot of $\langle w \rangle$ in (a). (c) Current modulation depth Γ (solid lines) as a function of the laser field ratio F_2/F_1 for different dc fields F_0. Dotted (dashed) lines in (c) are for the maximum (minimum) emission current density $\langle w \rangle$ at θ = 0 (θ = π). Here, the laser field F_1 is fixed as 1.8 V/nm.

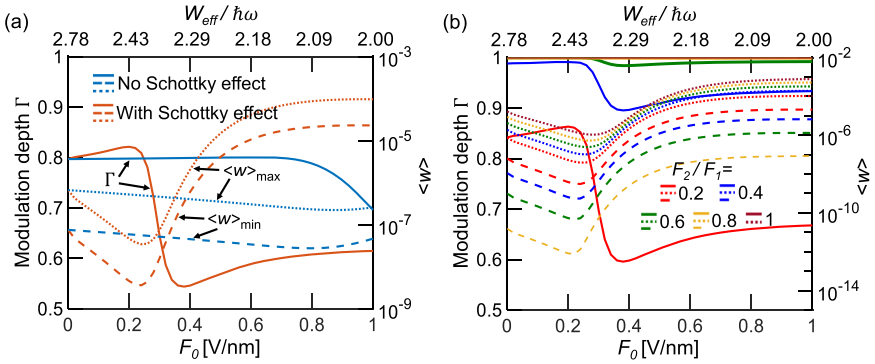

FIG. 3. (a) Emission current modulation depth Γ (solid lines) as a function of the dc field F_0 with and without the image-charge-induced potential barrier lowering (or the Schottky effect), for laser fields F_1 = 1.8 V/nm and F_2 = 0.3 V/nm. The case without the Schottky effect is calculated by replacing W_{eff} with the nominal work function of metal W in Eq. (1). (b) Modulation depth Γ (solid lines) as a function of F_0 for different laser field ratios F_2/F_1, with the effective work function W_{eff}. F_1 is fixed at 1.8 V/nm in (b). In (a) and (b), the dotted (dashed) lines are for the maximum (minimum) emission current density $\langle w \rangle$ at $\theta = 0$ ($\theta = \pi$).

current modulation depth Γ as a function of the dc field F_0 with and without the Schottky effect. When the Schottky effect is not considered, Γ gradually decreases with F_0. It is clear that the Schottky effect greatly alters the dependence of modulation depth Γ on the dc field F_0 [cf. solid lines in Fig. 3(a)]. The change in Γ originates from the change in the maximum (minimum) values of emission current $\langle w \rangle$ with the Schottky effect, as shown by dotted (dashed) lines in Fig. 3(a). As F_0 varies, the effective potential barrier W_{eff} changes, which induces an increase (decrease) in the emission current when the ratio $W_{eff}/\hbar\omega$ becomes closer to (further away from) an integer, where resonant n-photon absorption occurs (cf. Figs. 6 and 7 of Ref. 36). This resonant emission process causes the nonlinear behavior of Γ as a function of dc field F_0.

Figure 3(b) shows the modulation depth Γ as a function of the dc field F_0 for different laser field ratios F_2/F_1 with fixed F_1 = 1.8 V/nm. As F_2/F_1 approaches 1, the modulation depth Γ gradually approaches the maximum value of 1 for the full range of dc field F_0 from 0 V/nm to 1 V/nm. This is consistent with the observation in Fig. 2(c). Note that when F_0 is increased from 0 V/nm to 1 V/nm, the total emission current density can be increased by orders of magnitude.

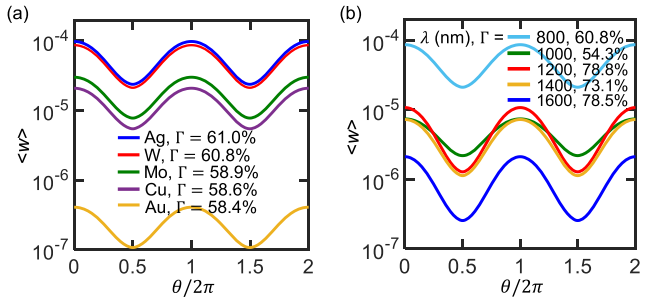

FIG. 4. Normalized total time-averaged emission current density $\langle w \rangle$ as a function of the phase difference θ, for various (a) cathode materials and (b) incident wavelengths. In (a), the laser wavelength λ = 800 nm ($\hbar\omega$ = 1.55 eV). The nominal work function of different materials is W_{Ag} = 4.26 eV,[42] W_W = 4.31 eV,[22,25] W_{Mo} = 4.6 eV,[42] W_{Cu} = 4.65 eV,[42] and W_{Au} = 5.1 eV.[36,42] In (b), the metal is tungsten. Here, the dc field F_0 is 0.8 V/nm, and the laser fields F_1 and F_2 are fixed at 1.8 V/nm and 0.3 V/nm, respectively.

We also examine the photoemission current modulation depth Γ for cathode materials with different work functions in Fig. 4(a) and for various incident laser wavelengths in Fig. 4(b). We fix the dc field F_0 = 0.8 V/nm and laser fields F_1 = 1.8 V/nm and F_2 = 0.3 V/nm. Under the same illumination condition, the electron emission current depends strongly on the work function; however, the modulation depth Γ varies only slightly. This is because Γ is predominantly determined by the ratio of the laser field strengths. Figure 4(b) shows the effect of the laser wavelength on both emission current and modulation depth for a tungsten cathode. The nonlinear dependence may also be attributed to the change in the ratio $W_{eff}/\hbar\omega$ near resonant n-photon processes.[36]

In summary, we propose to utilize two lasers of the same frequency to modulate the photoelectron emission by their phase delay. Compared to the two-color laser configuration, single-frequency laser pairs can be more easily implemented in experiments since they relax the requirement of higher order harmonic generation, which becomes increasingly difficult in the high laser intensity regimes. The intensity ratio of the single-frequency laser pairs can be tuned over a much wider range than the two-color laser system. We find that a strong current modulation (>90%) can be achieved with a moderate ratio of the laser fields (<0.4) even under a strong dc bias. The nonlinear effects of the dc field, cathode materials, and laser wavelength on both the emission current level and modulation depth are examined. The strong dependence of photoelectron energy spectra on the phase delay of the two lasers demonstrates promising potential for the application of time-resolved photoelectron spectroscopy using single-frequency laser pairs. Our study may inspire new routes toward many applications requiring both high photoemission current and strong current modulation, such as tabletop particle accelerators, photoelectron microscopy, and x-ray sources. Future research may consider the effects of cathode geometry, surface states and materials (e.g., semiconductor and two-dimensional materials), and different polarization and shape of laser pulses on photoelectron emission modulation. Further optical engineering techniques, such as those which may be provided by spatial light modulators (SLMs), might allow synthesis of even more

complex current waveforms in a compact experimental package. As SLMs have been demonstrated to operate at both high power and high energy, implementation in a variety of laser systems is possible.[43]

ACKNOWLEDGMENTS

This work was supported by Air Force Office of Scientific Research (AFOSR) YIP Grant No. FA9550-18-1-0061 and Office of Naval Research (ONR) YIP Grant No. N00014-20-1-2681.

DATA AVAILABLITY

The data that support the findings of this study are available within the article.

REFERENCES

[1] F. J. García de Abajo, Rev. Mod. Phys. **82**, 209 (2010).
[2] A. H. Zewail, Science **328**, 187 (2010).
[3] D.-S. Yang, O. F. Mohammed, and A. H. Zewail, Proc. Natl. Acad. Sci. U. S. A. **107**, 14993 (2010).
[4] A. Feist, N. Bach, N. Rubiano da Silva, T. Danz, M. Möller, K. E. Priebe, T. Domröse, J. G. Gatzmann, S. Rost, J. Schauss, S. Strauch, R. Bormann, M. Sivis, S. Schäfer, and C. Ropers, Ultramicroscopy **176**, 63 (2017).
[5] R. G. Hobbs, W. P. Putnam, A. Fallahi, Y. Yang, F. X. Kärtner, and K. K. Berggren, Nano Lett. **17**, 6069 (2017).
[6] V. A. Lobastov, J. Weissenrieder, J. Tang, and A. H. Zewail, Nano Lett. **7**, 2552 (2007).
[7] G. Sciaini and R. J. D. Miller, Rep. Prog. Phys. **74**, 096101 (2011).
[8] M. Gulde, S. Schweda, G. Storeck, M. Maiti, H. K. Yu, A. M. Wodtke, S. Schäfer, and C. Ropers, Science **345**, 200 (2014).
[9] M. Müller, A. Paarmann, and R. Ernstorfer, Nat. Commun. **5**, 1 (2014).
[10] P. Hommelhoff, Y. Sortais, A. Aghajani-Talesh, and M. A. Kasevich, Phys. Rev. Lett. **96**, 077401 (2006).
[11] C. Ropers, D. R. Solli, C. P. Schulz, C. Lienau, and T. Elsaesser, Phys. Rev. Lett. **98**, 043907 (2007).
[12] A. Polyakov, C. Senft, K. F. Thompson, J. Feng, S. Cabrini, P. J. Schuck, H. A. Padmore, S. J. Peppernick, and W. P. Hess, Phys. Rev. Lett. **110**, 076802 (2013).
[13] M. E. Swanwick, P. D. Keathley, A. Fallahi, P. R. Krogen, G. Laurent, J. Moses, F. X. Kärtner, and L. F. Velásquez-García, Nano Lett. **14**, 5035 (2014).
[14] P. G. O'Shea and H. P. Freund, Science **292**, 1853 (2001).
[15] I. Grguraš, A. R. Maier, C. Behrens, T. Mazza, T. J. Kelly, P. Radcliffe, S. Düsterer, A. K. Kazansky, N. M. Kabachnik, T. Tschentscher, J. T. Costello, M. Meyer, M. C. Hoffmann, H. Schlarb, and A. L. Cavalieri, Nat. Photonics **6**, 852 (2012).
[16] M. I. Stockman, M. F. Kling, U. Kleineberg, and F. Krausz, Nat. Photonics **1**, 539 (2007).
[17] M. Krüger, M. Schenk, and P. Hommelhoff, Nature **475**, 78 (2011).
[18] M. T. Hassan, J. Phys. B: At. Mol. Opt. Phys. **51**, 032005 (2018).
[19] P. Zhang and Y. Y. Lau, J. Plasma Phys. **82**, 595820505 (2016).
[20] P. Zhang, Á. Valfells, L. K. Ang, J. W. Luginsland, and Y. Y. Lau, Appl. Phys. Rev. **4**, 011304 (2017).
[21] J. Lin, P. Y. Wong, P. Yang, Y. Y. Lau, W. Tang, and P. Zhang, J. Appl. Phys. **121**, 244301 (2017).
[22] M. Förster, T. Paschen, M. Krüger, C. Lemell, G. Wachter, F. Libisch, T. Madlener, J. Burgdörfer, and P. Hommelhoff, Phys. Rev. Lett. **117**, 217601 (2016).
[23] W. C.-W. Huang, M. Becker, J. Beck, and H. Batelaan, New J. Phys. **19**, 023011 (2017).
[24] T. Paschen, M. Förster, M. Krüger, C. Lemell, G. Wachter, F. Libisch, T. Madlener, J. Burgdörfer, and P. Hommelhoff, J. Mod. Opt. **64**, 1054 (2017).
[25] L. Seiffert, T. Paschen, P. Hommelhoff, and T. Fennel, J. Phys. B: At. Mol. Opt. Phys. **51**, 134001 (2018).
[26] B. Ji, X. Song, Y. Dou, H. Tao, X. Gao, Z. Hao, and J. Lin, New J. Phys. **20**, 073031 (2018).
[27] Y. Luo and P. Zhang, Phys. Rev. B **98**, 165442 (2018).
[28] Y. Luo and P. Zhang, Phys. Rev. Appl. **12**, 044056 (2019).
[29] M. Reutzel, A. Li, and H. Petek, Phys. Rev. X **9**, 011044 (2019).
[30] P. Zhang and A. G. R. Thomas, Appl. Phys. Lett. **106**, 131102 (2015).
[31] E. C. Welch, P. Zhang, F. Dollar, Z.-H. He, K. Krushelnick, and A. G. R. Thomas, Phys. Plasmas **22**, 053104 (2015).
[32] A. L. Fymat, Appl. Opt. **10**, 2499 (1971).
[33] A. Rizea, Opto-Electron. Rev. **20**, 96 (2012).
[34] A. Rizea and I. M. Popescu, Rom. Rep. Phys. **64**, 482 (2012).
[35] S. G. Kaplan and M. A. Quijada, in *Experimental Methods in the Physical Sciences*, edited by T. A. Germer, J. C. Zwinkels, and B. K. Tsai (Academic Press, 2014), pp. 97–141.
[36] P. Zhang and Y. Y. Lau, Sci. Rep. **6**, 19894 (2016).
[37] Y. Zhou and P. Zhang, J. Appl. Phys. **127**, 164903 (2020).
[38] J. W. Gadzuk and E. W. Plummer, Rev. Mod. Phys. **45**, 487 (1973).
[39] S. V. Yalunin, M. Gulde, and C. Ropers, Phys. Rev. B **84**, 195426 (2011).
[40] P. Zhang, Sci. Rep. **5**, 9826 (2015).
[41] S. Banerjee and P. Zhang, AIP Adv. **9**, 085302 (2019).
[42] H. B. Michaelson, J. Appl. Phys. **48**, 4729 (1977).
[43] V. Bagnoud and J. D. Zuegel, Opt. Lett. **29**, 295 (2004).